An ankle-foot orthosis powered by artificial pneumatic muscles

Daniel P. Ferris[1,2]*, Joseph M. Czerniecki[3,5], and Blake Hannaford[4]

Departments of [1]Movement Science and [2]Biomedical Engineering, University of Michigan, Ann Arbor, MI; Departments of [3]Rehabilitation Medicine and [4]Electrical Engineering, University of Washington, Seattle, WA; [5]VA Puget Sound Healthcare System, Seattle, WA

*Corresponding author:
Daniel P. Ferris
University of Michigan
401 Washtenaw Ave.
Ann Arbor, MI 48109-2214
e-mail: ferrisdp@umich.edu
Phone: (734) 647-6878
Fax: (734) 936-1925

Keywords: locomotion, exoskeleton, gait, rehabilitation, proportional myoelectric control

Abstract

Our goal was to develop a powered orthosis for the lower limb that could comfortably provide external torque during human walking. We constructed the orthosis from a carbon fiber shell with hinge joint and two artificial pneumatic muscles. One artificial pneumatic muscle provided plantar flexion torque and one artificial pneumatic muscle provided dorsiflexion torque. We collected joint kinematic and artificial muscle force data as one healthy subject walked with the orthosis using proportional myoelectric control. Peak plantar flexor torque provided by the orthosis was 70 Nm and peak dorsiflexor torque provided by the orthosis was 38 Nm. Soleus and tibialis anterior EMG amplitudes changed in response to powered orthosis assistance. Future studies could use similiar powered orthoses to study biomechanics and motor adaptation during human walking or to assist gait rehabilitation after neurological injury.

1. Introduction

Research on wearable robotic devices to assist human movement has greatly expanded in recent years. This has partially been a result of the Defense Advanced Research Projects Agency (DARPA) program on exoskeletons for human performance augmentation. DARPA's long-term goal is to build exoskeletons that can improve soldier endurance, speed, and load carrying ability (Fanelli, 2001; Lemley, 2002; Weiss, 2001). Presumably, exoskeletons that could augment human performance in this manner would also benefit civilian laborers such as firefighters, construction workers, and warehouse personnel.

Scientists and engineers are also working on robotic exoskeletons to aid individuals after neurological injury. Recent breakthroughs in clinical neuroscience have revealed that humans with spinal cord injury or stroke can increase their motor capabilities through intense task-specific practice (Barbeau et al., 1998; Dietz et al., 1998; Harkema, 2001; Wernig et al., 1995). For gait rehabilitation, locomotor training often requires the manual assistance of three or more physical therapists and a harness to provide partial body weight support (Behrman and Harkema, 2000). Robotic exoskeletons or powered orthoses could reduce therapist manual labor and increase the consistency of locomotor training. One device that is commercially available, the Lokomat (Colombo et al., 2000; Jezernik et al., 2003), is currently being tested in multiple sites across Europe and North America. The Lokomat uses four electrical motors to assist hip and knee movement as the patient steps on a treadmill. Other research groups are developing similar robotic devices for repetitive step training (Edgerton et al., 2001; Hesse et al., 2000; Reinkensmeyer, 2003). Importantly, all of these devices are intended to assist patients while stepping in place on a treadmill or

elliptical trainer. In addition, none of them provide plantar flexion torque at the ankle. The lack of plantar flexion torque could be a particularly significant aspect. The plantar flexor muscles provide more positive mechanical work than the knee or hip during normal walking (Gitter et al., 1991). Although the specific functions of the plantar flexors are controversial, there is evidence that they contribute to support, propulsion, swing leg acceleration, and decreasing collisions at heel contact (Donelan et al., 2002; Gitter et al., 1991; Gottschall and Kram, 2003; Hof et al., 1992; Kuo, 2002; Meinders et al., 1998; Neptune et al., 2001; Neptune et al., 2004; Winter, 1983).

Our goal was to develop a lightweight powered orthosis for the lower limb that could comfortably provide plantar flexion and dorsiflexion assistance during human walking. The powered orthosis was intended to be used for basic locomotion studies in a laboratory or for gait rehabilitation in a clinic. As a result, a self-contained computer controller and energy supply were not necessary. We constructed the orthosis using a carbon fiber shell and artificial pneumatic muscles, and tested the orthosis on a single subject using proportional myoelectric control. Because we wanted to ensure that the orthosis was comfortable during extended wear, the subject walked for thirty minutes of continuous treadmill walking with the powered orthosis. We chose this length of time because it was similar to previous gait studies examining the effects of audio-visual biofeedback (Colborne and Olney, 1990; Colborne et al., 1993; Colborne et al., 1994). We collected data for powered plantar flexion and powered dorsiflexion separately because we wanted to examine the independent effects of each artificial muscle without co-activation as a confounding factor.

2. Methods

Frame

We constructed the orthosis frame from carbon fiber (Figure 1). We chose carbon fiber for its strength and low specific weight. After taking a cast of the subject's lower limb, an orthotist fabricated the shell through carbon fiber lamination. Plastic Oklahoma joints connected the upper shank portion of the ankle-foot orthosis with the lower foot section. Titanium fittings with threaded holes (i.e. prosthesis pyramids) were laminated directly into the shell between layers of carbon fiber weave. The fittings allowed us to rigidly attach actuators to the orthosis using steel ball joint rod ends (M10 x 1.5 mm) (McMaster-Carr, Los Angeles, CA) screwed into the threads of the fittings.

Actuators

For the actuators, we used pneumatic artificial muscles due to their low weight and high power output. Artificial pneumatic muscles were studied as power sources for upper extremity orthoses during the 1950's and 1960's (Geddes et al., 1959; Nickel et al., 1963; Schulte, 1961). They are sometimes referred to as McKibben artificial muscles or braided pneumatic muscle actuators. In recent years there has been a resurgence in their use in robotics (Caldwell et al., 2000; Klute et al., 2002; Tondu and Lopez, 2000). Their high power to weight ratios and natural compliance make them particularly well-suited for human-machine interactions such as virtual reality force feedback (Brown et al., 2003; Tsagarakis et al., 1999), human power augmentation (Brown et al., 2003; Umetani et al., 1999), and rehabilitation (Noritsugu and Tanaka, 1997; Prior et al., 1993; Repperger et al., 1997; Tsagarakis and Caldwell, 2003).

Artificial pneumatic muscles consist of an expandable internal bladder surrounded by a braided shell. When the internal bladder is pressurized, it expands in a balloon-like manner. The braided shell constrains the expansion and maintains a cylindrical shape. As the volume of the internal bladder increases with increasing pressure, the muscle shortens and/or produces tension if coupled to a mechanical load. Recent studies have quantified the force-length, force-velocity, force-activation, and bandwidth properties of artificial pneumatic muscles in detail (Davis et al., 2003; Klute et al., 2002; Klute and Hannaford, 2000; Reynolds et al., 2003). The force produced by the muscle decreases as a function of muscle length. The muscles are longest at rest and cannot be stretched beyond this length. They shorten approximately one-third of their resting length at maximum contraction. The muscles have an inherent elastic component that stores and returns elastic energy during stretch-shortening cycles.

We constructed the artificial pneumatic muscles using latex tubing for the inner bladder (1.3 mm inner diameter, 2.4 mm wall), braided polyester sleeving for the muscle shell (31.8 mm width), plastic pneumatic fittings for the endcaps and nozzles (4.9 mm by 6.4 mm NPT), and double ear hose clamps to seal the endcaps and nozzles in the tubing and sleeving (McMaster-Carr, Los Angeles, CA). We cut the sleeving and folded it back on itself before sealing the hose clamp in order to provide an attachment loop. Steel wire (20 gauge) transmitted force from the sleeving loops to the rod ends. A tension load sensor (LC-202, Omega Engineering, Inc., Stamford, CT) was between the muscle and the rod end to measure the force in the muscle. Clear nylon tubing (4.8 mm inner diameter, 1.6 mm wall, 6 m length) supplied compressed air to the muscles (0-4.8 bar) from a proportional pressure regulator (MPP-3-1/8, Festo Corporation, Hauppauge, N.Y.).

The ankle-foot orthosis had a total mass, including artificial muscles and force transducers, of 1.6 kg for a 100 kg subject. For comparison, regression equations estimate foot and shank mass to be 5.4 kg for a 100 kg subject (Chandler et al., 1975). We considered this mass acceptable because previous research had found that adding a 1.82 kg ankle weight to one limb in ten healthy subjects did not significantly alter freely chosen walking speed, gait cadence, stride length, or rate of oxygen consumption (Barnett et al., 1993). The powered ankle-foot orthosis distributed the mass of the orthosis over the entire length of the foot and shank instead of being concentrated about the ankle joint so effects should also be attenuated.

Control System

Proportional myoelectric control uses the body's own muscle activation signals to control external devices. Engineers have employed proportional myoelectrical control for many years as a means for operating powered upper extremity prostheses (Hogan, 1976; Parker and Scott, 1986; Sears and Shaperman, 1991). This method provides a direct link between biological muscle activation and artificial muscle force, facilitating motor learning by the wearer.

We implemented proportional myoelectrical control through a desktop personal computer and a real-time control board (ACE Kit 1103, dSPACE, Inc., Northville, MI). The software program was written in Simulink (The Mathworks, Inc., Natick, MA) and converted to ControlDesk (dSPACE, Inc., Northville, MI). The program regulated air pressure in the artificial pneumatic muscles proportional to the processed muscle activation pattern in real time. EMG signals from the soleus and tibialis anterior were first high-pass filtered with a second order Butterworth filter (f_c = 20 Hz) to remove

movement artifact. Then the signals were full wave rectified and low-pass filtered with a second order Butterworth filter (f_c = 10 Hz) to smooth the signal. After passing through a threshold cutoff to eliminate background noise and an adjustable gain to scale the signal, the software sent a 0-10 V analog signal to the proportional pressure regulator. The relationship between EMG amplitude and artificial pneumatic muscle force was non-linear due to force-length properties and activation dynamics of the pneumatic muscles (Davis et al., 2003; Klute et al., 2002; Klute and Hannaford, 2000; Reynolds et al., 2003).

Bench Top Testing

We measured the activation dynamics of the artificial muscles in isometric conditions on a bench top to compare them to human muscle. Using a function generator, we sent a single 5 ms square pulse into the analog to digital board of the personal computer to activate the artificial pneumatic muscle. The control software converted the pulse into a control signal as described previously and we recorded tension in the artificial pneumatic muscle. We used a zero threshold and the smallest gain that produced a clear twitch in artificial pneumatic muscle force. We also used soleus EMG to activate the artificial muscles on the bench top to calculate electromechanical delay with proportional myoelectric control (i.e. time from onset of soleus EMG burst to increase in artificial pneumatic muscle force).

Subject Testing

One healthy subject (age 31 years, body mass 100 kg) walked with the orthosis to test its performance during gait. We collected three-dimensional joint kinematics (60

Hz, Peak Motus, Peak Performance Technologies, Inc., Centennial, CO) and lower limb electromyography from the soleus and tibialis anterior (1200 Hz, Telemyo, Noraxon USA, Inc., Scottsdale, AZ) as the subject walked on a treadmill at 1.2 m/s. For the proportional myoelectric control, we set the threshold to 25 μV. We adjusted the gain to produce a control signal that would have a brief maximum of 10 volts based on the EMG pattern demonstrated while walking with the passive orthosis. To calculate joint angle displacement, we smoothed marker position data with a fourth order Butterworth low-pass filter (f_c = 6 Hz) with zero lag. Bandwidth of the EMG amplifier was 20-500 Hz. After data collection, we processed the raw EMG signals with a second order Butterworth high-pass filter (f_c = 20 Hz) with zero time lag, full wave rectification, and then averaged together five consecutive stride cycles. We determined time of heel strike from heel marker vertical position data.

The subject walked under four different test conditions. We first collected data without the orthosis (6 minutes of continuous walking) and with the orthosis passive (6 minutes of continuous walking). For the third condition, soleus EMG controlled the artificial plantar flexor and the artificial dorsiflexor was not attached to the orthosis (30 minutes of continuous walking). After the third condition, the subject walked with the orthosis passive again (15 minutes of continuous walking). For the fourth condition, tibialis anterior EMG controlled the artificial dorsiflexor and the artificial plantar flexor was not attached to the orthosis (30 minutes of continuous walking). After the fourth conditions, the subject again walked on the treadmill while wearing the orthosis passive (15 minutes of continuous walking).

3. Results

Bench Top Testing

Activation dynamics of the artificial pneumatic muscles were similar to those of human muscle. For the artificial pneumatic muscle twitch tests (Figure 2), we calculated a time to peak tension of 72 ± 5 ms and a half relaxation time of 81 ± 7 ms (mean ± s.d.). Respective values for human triceps surae are 101 ms and 94 ms (Rice et al., 1988) and for human tibialis anterior are 99 ms and 87 ms (Connelly et al., 1999). The artificial pneumatic muscles had an electromechanical delay of 47 ± 7 ms between EMG burst onset and initial rise in artificial muscle tension (mean ± s.d.). Analogous measurements on human muscle indicate electromechanical delay values for human soleus and gastrocnemius are 27 ms and 35 ms, respectively (Komi et al., 1987). We could not find data in the literature showing electromechanical delay values for human tibialis anterior that recorded muscle force directly from the tendon. Although electromechanical delay for the artificial pneumatic muscles is slightly longer than for human muscle, the difference is counterbalanced by slightly faster twitch mechanics for the artificial pneumatic muscles.

Subject Testing

The ankle-foot orthosis was comfortable to wear and did not interfere with walking when worn passively. Muscle activation patterns were very similar between walking with no orthosis and walking with the passive orthosis (Figure 3). There was slightly less ankle dorsiflexion during the beginning of the swing phase, but most joint kinematic profiles were remarkably similar for no orthosis and passive orthosis conditions. It appeared that the subject had easily accommodated to its added mass within six minutes of walking on a treadmill.

When the artificial plantar flexor powered the orthosis, it provided a large plantar flexor torque during stance (Figure 4). Peak torque provided by the orthosis was 70 Nm for the first minute of powered plantar flexion (Figure 4A). Peak dorsiflexion angle during stance was slightly less and occurred earlier in the stride cycle for the first minute of walking with powered plantar flexion compared to walking with the passive orthosis (7 degrees and 47% vs. 15 degrees and 53%, respectively). After thirty minutes of walking with powered plantar flexion (Figure 4B), peak plantar flexor torque, peak dorsiflexion angle, and peak dorsiflexion timing (66 Nm, 8 degrees, and 48%, respectively) were similar to the first minute of powered plantar flexion. Soleus muscle activation amplitude during the thirty minutes of powered plantarflexion averaged 53% of the amplitude during passive orthosis walking (Figure 6A). Tibialis anterior activation amplitude during powered plantar flexion averaged 10% higher than the passive orthosis condition. After turning off the orthosis at the end of thirty minutes, muscle activation amplitudes and joint kinematic profiles quickly returned to the passive orthosis baseline values collected prior to powered plantarflexion (Figure 6A).

When the artificial dorsiflexor powered the orthosis, the added dorsiflexor torque decreased plantar flexion during early stance and throughout the swing phase (Figure 5). For the first minute of powered dorsiflexion (Figure 5A), peak torque provided by the orthosis was 38 Nm during early stance and 8 Nm during the stance to swing transition. As a result, peak plantar flexion during the first minute of powered dorsiflexion was 9 degrees less during early stance and 12 degrees less during the swing phase compared to the passive condition. After thirty minutes of walking (Figure 5B), peak dorsiflexion torques (38 Nm during early stance and 6 Nm during the stance to swing transition) were similar to the first minute of powered dorsiflexion. However, peak plantar flexion

after thirty minutes of walking was only 7 degrees less than the passive orthosis condition during early stance and only 6 degrees less than the passive orthosis condition during swing. Tibialis anterior muscle activation during thirty minutes of powered dorsiflexion averaged 80% of the passive orthosis condition (Figure 6B). Soleus muscle activation amplitude was 82% of the passive orthosis condition during the first minute of powered dorsiflexion, but steadily increased during the thirty minute of walking. By the end of the powered dorsiflexion, soleus EMG was 110% of the passive orthosis condition. Similar to the powered plantar flexion tests, muscle activation amplitudes and joint kinematic profiles quickly returned to baseline after turning off the orthosis (Figure 6B).

4. Discussion

The study demonstrated that is feasible to construct a lightweight powered orthosis providing substantial external torque to the ankle joint during human walking. The artificial pneumatic muscles are powerful actuators with mechanical properties similar to human muscle. Based on normative data from the literature (Alkjaer et al., 2001; Sadeghi et al., 2001) and the subject's body mass, the powered orthosis was able to provide about 50% of the peak plantar flexor net muscle moment and about 400% of the peak dorsiflexor net muscle moment during unassisted walking.

Although data were only for one subject, they suggest that humans can quickly modify muscle activation amplitudes to accommodate powered assistance during walking. Joint kinematic patterns were fairly robust across the experiment. Kinematic differences between powered and passive orthosis walking decreased with thirty minutes of walking (Figures 4 and 5). These observations support the hypothesis that

muscle activation patterns are fairly plastic during gait (Pearson, 2000) and that the nervous system may plan lower limb movements through kinematic trajectories (Lacquaniti et al., 1999).

We used proportional myolectric control from synergistic muscles for our data collection, but it would be easy and scientifically interesting to use alternative types of control. For example, using proportional myoelectric control from soleus EMG to an artificial dorsiflexor would provide co-activation about the ankle joint similar to that seen in many neurological disorders (e.g. stroke). Studying how neurologically intact humans walk with altered neuromechanical states could aid in the development of new gait rehabilitation strategies. Controllers based on gait kinematics or adaptive algorithms (Ferris et al., 2002) could be helpful in assisting locomotor training after spinal cord injury or stroke (Edgerton et al., 2001). Blaya and Herr (Blaya and Herr, 2004) have recently demonstrated that an adaptive impedance controller for powered dorsiflexion torque has good potential for aiding patients with drop-foot.

From a more general, basic science perspective, we have little understanding of how powered locomotor assistance will affect the biomechanics and energetics of human locomotion. Historically, exoskeleton researchers have focused on hardware and control methods (Hughes, 1972; Kazerooni, 1995; Kazerooni, 1996; Kazerooni and Jenhwa, 1993; Ruthenberg et al., 1997; Seireg and Grundman, 1981; Vukobratovic, 1973; Vukobratovic et al., 1990; Vukobratovic et al., 1970; Vukobratovic et al., 1974; Vukobratovic and Stokic, 1980). Little attention has been devoted to human motor adaptation with lower limb powered assistance. In addition, no study has ever measured metabolic cost of a subject walking with a powered exoskeleton. This seems quite remarkable given that the one of the primary goals of human augmentation

exoskeletons is to decrease effort and energy expenditure of humans. How much metabolic energy could a human save while wearing a robotic exoskeleton? What level of mechanical power output is necessary for an exoskeleton to be useful? Which lower limb joint is most important for reducing metabolic energy cost? Using pneumatically powered orthoses such as the one developed in this study, it may be possible to answer these questions with carefully controlled experimental studies.

Acknowledgments

This research was supported by NIH AR08602, NIH NS045486, and United States Department of Veterans Affairs Center Grant #A0806C. The authors greatly appreciated the help of Kristen Jaax, Glenn Klute, Jocelyn Berge, and Eric Rohr. We would especially like to thank Martin McDowell, C.P.O., for fabricating the carbon fiber shell.

References

Alkjaer, T., Simonsen, E.B., Dyhre-Poulsen, P., 2001. Comparison of inverse dynamics calculated by two- and three-dimensional models during walking. Gait & Posture 13, 73-77.

Barbeau, H., Norman, K., Fung, J., Visintin, M., Ladouceur, M., 1998. Does neurorehabilitation play a role in the recovery of walking in neurological populations? Annals of the New York Academy of Sciences 860, 377-392.

Barnett, S.L., Bagley, A.M., Skinner, H.B., 1993. Ankle weight effect on gait: orthotic implications. Orthopedics 16, 1127-1131.

Behrman, A.L., Harkema, S.J., 2000. Locomotor training after human spinal cord injury: a series of case studies. Physical Therapy 80, 688-700.

Blaya, J.A., Herr, H., 2004. Adaptive control of a variable-impedance ankle-foot orthosis to assist drop-foot gait. IEEE Transactions on Neural Systems and Rehabilitation Engineering 12, 24-31.

Brown, M., Tsagarakis, N., Caldwell, D.G., 2003. Exoskeletons for human force augmentation. Industrial Robot 30, 592-602.

Caldwell, D.G., Tsagarakis, N., Medrano Cerda, G.A., 2000. Bio-mimetic actuators: polymeric pseudo muscular actuators and pneumatic muscle actuators for biological emulation. Mechatronics 10, 499-530.

Chandler, R.F., Clauser, C.E., McConville, J.T., Reynolds, H.M., Young, J.W. (1975) Investigation of inertial properties of the human body (AMRL-TR-74-137). Aerospace Medical Research Laboratories, Wright-Patterson Air Force Base, OH.

Colborne, G.R., Olney, S.J., 1990. Feedback of joint angle and EMG in gait of able-bodied subjects. Archives of Physical Medicine and Rehabilitation 71, 478-483.

Colborne, G.R., Olney, S.J., Griffin, M.P., 1993. Feedback of ankle joint angle and soleus electromyography in the rehabilitation of hemiplegic gait. Archives of Physical Medicine and Rehabilitation 74, 1100-1106.

Colborne, G.R., Wright, F.V., Naumann, S., 1994. Feedback of triceps surae EMG in gait of children with cerebral palsy: a controlled study. Archives of Physical Medicine and Rehabilitation 75, 40-45.

Colombo, G., Joerg, M., Schreier, R., Dietz, V., 2000. Treadmill training of paraplegic patients using a robotic orthosis. Journal of Rehabilitation Research and Development 37, 693-700.

Connelly, D.M., Rice, C.L., Roos, M.R., Vandervoort, A.A., 1999. Motor unit firing rates and contractile properties in tibialis anterior of young and old men. Journal of Applied Physiology 87, 843-852.

Davis, S., Tsagarakis, N., Canderle, J., Caldwell, D.G., 2003. Enhanced modelling and performance in braided pneumatic muscle actuators. International Journal of Robotics Research 22, 213-227.

Dietz, V., Wirz, M., Colombo, G., Curt, A., 1998. Locomotor capacity and recovery of spinal cord function in paraplegic patients: A clinical and electrophysiological evaluation. Electroencephalography and Clinical Neurophysiology 109, 140-153.

Donelan, J.M., Kram, R., Kuo, A.D., 2002. Mechanical work for step-to-step transitions is a major determinant of the metabolic cost of human walking. Journal of Experimental Biology 205, 3717-3727.

Edgerton, V.R., Leon, R.D., Harkema, S.J., Hodgson, J.A., London, N., Reinkensmeyer, D.J., Roy, R.R., Talmadge, R.J., Tillakaratne, N.J., Timoszyk, W., Tobin, A., 2001. Retraining the injured spinal cord. Journal of Physiology (London) 533, 15-22.

Fanelli, S., 2001. Power dressing. New Scientist, 33-35.

Ferris, D.P., Viant, T.L., Campbell, R.J., 2002. Artificial neural oscillators as controllers for locomotion simulations and robotic exoskeletons. *IVth World Congress of Biomechanics*, Calgary, Alberta.

Geddes, L.A., Moore, L.G., Spencer, W.A., Hoff, H.E., 1959. Electro-pneumatic control of the McKibben synthetic muscle. Orthopedic and Prosthetic Appliance Journal 13, 33-36.

Gitter, A., Czerniecki, J.M., DeGroot, D.M., 1991. Biomechanical analysis of the influence of prosthetic feet on below-knee amputee walking. American Journal of Physical Medicine and Rehabilitation 70, 142-148.

Gottschall, J.S., Kram, R., 2003. Energy cost and muscular activity required for propulsion during walking. Journal of Applied Physiology 94, 1766-1772.

Harkema, S.J., 2001. Neural plasticity after human spinal cord injury: application of locomotor training to the rehabilitation of walking. Neuroscientist 7, 455-468.

Hesse, S., Uhlenbrock, D., Werner, C., Bardeleben, A., 2000. A mechanized gait trainer for restoring gait in nonambulatory subjects. Archives of Physical Medicine and Rehabilitation 81, 1158-1161.

Hof, A.L., Nauta, J., Vanderknaap, E.R., Schallig, M.A.A., Struwe, D.P., 1992. Calf Muscle Work and Segment Energy Changes in Human Treadmill Walking. Journal of Electromyography and Kinesiology 2, 203-216.

Hogan, N., 1976. A review of the methods of processing EMG for use as a proportional control signal. Biomedical Engineering 11, 81-86.

Hughes, J., 1972. Powered lower limb orthotics in paraplegia. Paraplegia 9, 191-193.

Jezernik, S., Scharer, R., Colombo, G., Morari, M., 2003. Adaptive robotic rehabilitation of locomotion: a clinical study in spinally injured individuals. Spinal Cord 41, 657-666.

Kazerooni, H., 1995. The Extender Technology at the University of California, Berkeley. Journal of the Society of Instrument and Control Engineers 34, 291-298.

Kazerooni, H., 1996. The human power amplifier technology at the University of California, Berkeley. Robotics and Autonomous Systems 19, 179-187.

Kazerooni, H., Jenhwa, G., 1993. Human extenders. Transactions of the ASME Journal of Dynamic Systems, Measurement and Control 115, 281-290.

Klute, G.K., Czerniecki, J.M., Hannaford, B., 2002. Artificial muscles: Actuators for biorobotic systems. International Journal of Robotics Research 21, 295-309.

Klute, G.K., Hannaford, B., 2000. Accounting for elastic energy storage in McKibben artificial muscle actuators. Journal of Dynamic Systems, Measurement and Control 122, 386-388.

Komi, P.V., Salonen, M., Jarvinen, M., Kokko, O., 1987. In vivo registration of achilles tendon forces in man 1. methodological development. International Journal of Sports Medicine 8, 3-8.

Kuo, A.D., 2002. Energetics of actively powered locomotion using the simplest walking model. Journal of Biomechanical Engineering 124, 113-120.

Lacquaniti, F., Grasso, R., Zago, M., 1999. Motor patterns in walking. News in Physiological Sciences 14, 168-174.

Lemley, B., 2002. Future tech: really special forces. Discover 23, 25-26.

Meinders, M., Gitter, A., Czerniecki, J.M., 1998. The role of ankle plantar flexor muscle work during walking. Scandinavian Journal of Rehabilitation Medicine 30, 39-46.

Neptune, R.R., Kautz, S.A., Zajac, F.E., 2001. Contributions of the individual ankle plantar flexors to support, forward progression and swing initiation during walking. Journal of Biomechanics 34, 1387-1398.

Neptune, R.R., Zajac, F.E., Kautz, S.A., 2004. Muscle force redistributes segmental power for body progression during walking. Gait and Posture 19, 194-205.

Nickel, V.L., Perry, J., Garrett, A.L., 1963. Development of useful function in the severly paralyzed hand. Journal of Bone and Joint Surgery 45, 933-952.

Noritsugu, T., Tanaka, T., 1997. Application of rubber artificial muscle manipulator as a rehabilitation robot. Ieee-Asme Transactions on Mechatronics 2, 259-267.

Parker, P.A., Scott, R.N., 1986. Myoelectric control of prostheses. Critical Reviews in Biomedical Engineering 13, 283-310.

Pearson, K.G., 2000. Neural adaptation in the generation of rhythmic behavior. Annual Review of Physiology 62, 723-753.

Prior, S.D., Warner, P.R., White, A.S., Parsons, J.T., Gill, R., 1993. Actuators for rehabilitation robots. Mechatronics 3, 285-294.

Reinkensmeyer, D.J., 2003. Rehabilitators. In *Standard Handbook of Biomedical Engineering & Design* (Edited by Kutz, M.), pp. 35.31-35.17. McGraw-Hill.

Repperger, D.W., Phillips, C.A., Johnson, D.C., Harmon, R.D., Johnson, K., 1997. A study of pneumatic muscle technology for possible assistance in mobility. *International Conference of the IEEE Engineering in Medicine and Biology Society*, Chicago, IL, USA, 1884-1887.

Reynolds, D.B., Repperger, D.W., Phillips, C.A., Bandry, G., 2003. Modeling the dynamic characteristics of pneumatic muscle. Annals of Biomedical Engineering 31, 310-317.

Rice, C.L., Cunningham, D.A., Taylor, A.W., Paterson, D.H., 1988. Comparison of the histochemical and contractile properties of human triceps surae. European Journal of Applied Physiology and Occupational Physiology 58, 165-170.

Ruthenberg, B.J., Wasylewski, N.A., Beard, J.E., 1997. An experimental device for investigating the force and power requirements of a powered gait orthosis. Journal of Rehabilitation Research and Development 34, 203-213.

Sadeghi, H., Sadeghi, S., Prince, F., Allard, P., Labelle, H., Vaughan, C.L., 2001. Functional roles of ankle and hip sagittal muscle moments in able-bodied gait. Clinical Biomechanics 16, 688-695.

Schulte, H.F., 1961. The characteristics of the McKibben artificial muscle. In *The Application of External Power in Prosthetics and Orthotics* (Edited), pp. H:94-115. National Academy of Sciences - National Research Council, Washington, DC.

Sears, H.H., Shaperman, J., 1991. Proportional myoelectric hand control: an evaluation. American Journal of Physical Medicine and Rehabilitation 70, 20-28.

Seireg, A., Grundman, J.G., 1981. Design of a multitask exoskeletal walking device for paraplegics. In *Biomechanics of Medical Devices* (Edited by Ghista, D. N.), pp. 569-639. Marcel Dekker, Inc., New York.

Tondu, B., Lopez, P., 2000. Modeling and control of McKibben artificial muscle robot actuators. IEEE Control Systems Magazine 20, 15-38.

Tsagarakis, N., Caldwell, D.G., Medrano-Cerda, G.A., 1999. A 7 DOF pneumatic muscle actuator (pMA) powered exoskeleton. *IEEE International Workshop on Robot and Human Interaction*, Pisa, Italy, 327-333.

Tsagarakis, N.G., Caldwell, D.G., 2003. Development and control of a 'soft-actuated' exoskeleton for use in physiotherapy and training. Autonomous Robots 15, 21-33.

Umetani, Y., Yamada, Y., Morizono, T., Yoshida, T., Aoki, S., 1999. "Skil Mate" wearable exoskeleton robot. *IEEE International Conference on Systems, Man and Cybernetics*, Tokyo, Japan, 984-988.

Vukobratovic, M., 1973. How to control artificial anthropormorphic systems. IEEE Transactions on Systems, Man and Cybernetics 3, 497-507.

Vukobratovic, M., Borovac, B., Surla, D., Stokic, D., 1990. Biped Locomotion: Dynamics, Stability, Control and Application. Springer-Verlag, Berlin.

Vukobratovic, M., Frank, A.A., Juricic, D., 1970. On the stability of biped locomotion. IEEE Transactions on Biomedical Engineering 17, 25-36.

Vukobratovic, M., Hristic, D., Stojiljkovic, Z., 1974. Development of active anthropomorphic exoskeletons. Medicine and Biology in Engineering 12, 66-80.

Vukobratovic, M., Stokic, D., 1980. Significance of force-feedback in controlling artificial locomotion-manipulation systems. IEEE Transactions on Biomedical Engineering 27, 705-713.

Weiss, P., 2001. Dances with robots. Science News 159, 407-408.

Wernig, A., Muller, S., Nanassy, A., Cagol, E., 1995. Laufband therapy based on 'rules of spinal locomotion' is effective in spinal cord injured persons. European Journal of Neuroscience 7, 823-829.

Winter, D.A., 1983. Energy generation and absorption at the ankle and knee during fast, natural, and slow cadences. Clinical Orthopaedics, 147-154.

Figure Captions

Figure 1. **Powered Ankle-Foot Orthosis.** The carbon fiber shell has an artificial pneumatic dorsiflexor (maximally inflated) and artificial pneumatic plantar flexor (relaxed) attached via titanium fittings. Load cells in series with the artificial muscles recorded muscle tension. Dorsiflexor moment arm varied from 14 to 16 cm and plantar flexor moment arm was 10 cm for the range of motion during walking.

Figure 2. Artificial Muscle Twitch. A 5 ms Input pulse triggered a Control Signal to the proportional pressure regulator, resulting in an artificial muscle twitch. We elicited the twitches during isometric bench top tests.

Figure 3. Comparison of muscle activation patterns and joint kinematics for no orthosis and passive orthosis conditions. Mean EMG and joint angle profiles were not substantially different between walking with no orthosis (black lines) and walking with the passive orthosis (grey lines). The most noticeable difference was slightly less dorsiflexion during swing when wearing the passive orthosis. EMG graphs include mean profiles of both conditions. Joint angle graphs include mean profiles of the no orthosis condition (±1 S.D.) and mean profiles of the passive orthosis condition. Zero degrees represents standing posture. Flexion is positive for the knee and hip joint graphs. Plantar flexion is positive for the ankle joint graph.

Figure 4. **Comparison of muscle activation patterns and joint kinematics for passive orthosis and powered plantar flexor orthosis conditions.** Soleus recruitment produced the Control Signal activating the artificial plantar flexor. Powered condition in A is after one minute of wearing the orthosis and powered condition in B is after 30 minutes of wearing the orthosis (both black lines). Passive condition in both A and B is after 6 minutes of wearing the orthosis (grey lines). Soleus EMG amplitude was substantially lower during walking with the powered plantar flexor compared to during walking with the passive orthosis. The ankle joint underwent less dorsiflexion during late stance when the orthosis was powered by the artificial plantar flexor. EMG graphs include mean profiles of both conditions. Control signal, artificial muscle force, and joint angle graphs include mean profiles of the powered orthosis condition (±1 SD) and mean profiles of the passive orthosis condition. Zero degrees represents standing posture. Flexion is positive for the knee and hip joint graphs. Plantarflexion is positive for the ankle joint graph.

Figure 5. **Comparison of muscle activation patterns and joint kinematics for passive orthosis and powered dorsiflexor orthosis conditions.** Tibialis anterior recruitment produced the Control Signal activating the artificial dorsiflexor. Powered condition in A is after one minute of wearing the orthosis and powered condition in B is after 30 minutes of wearning the orthosis (both black lines). Passive condition in both A and B is after 6 minutes of wearing the orthosis (grey lines). Tibialis anterior EMG amplitude was slightly lower during walking with the powered dorsiflexor compared to during walking with the passive orthosis. The ankle joint underwent less plantar flexion during early stance and early swing when the orthosis was powered by the artificial dorsiflexor. EMG graphs include mean profiles of both conditions. Control signal, artificial muscle force, and joint angle graphs include mean profiles of the powered

orthosis condition (±1 SD) and mean profiles of the passive orthosis condition. Zero degrees represents standing posture. Flexion is positive for the knee and hip joint graphs. Plantar flexion is positive for the ankle joint graph.

Figure 6. Muscle activation amplitudes. A) During walking with powered plantar flexion (PPF), soleus EMG (circles) decreased to approximately one half the value seen during the passive orthosis condition. Tibialis anterior EMG (squares) remained fairly stable, with only a small increase during powered plantar flexion compared to passive orthosis walking. Both muscles returned quickly to the baseline amplitudes after the orthosis was turned off. B) During walking with powered dorsiflexion (PDF), tibialis anterior EMG (squares) decreased slightly compared to the passive orthosis condition. Soleus EMG (circles) did not change much during powered dorsiflexion compared to walking with the passive orthosis. Points represent the average root mean square amplitude (RMS) of five consecutive stride cycles. Standard error bars are smaller than the symbols.

Figure 1. Powered Ankle-Foot Orthosis. The carbon fiber shell has an artificial pneumatic dorsiflexor (maximally inflated) and artificial pneumatic plantar flexor (relaxed) attached via titanium fittings. Load cells in series with the artificial muscles recorded muscle tension. Dorsiflexor moment arm varied from 14 to 16 cm and plantar flexor moment arm was 10 cm for the range of motion during walking.

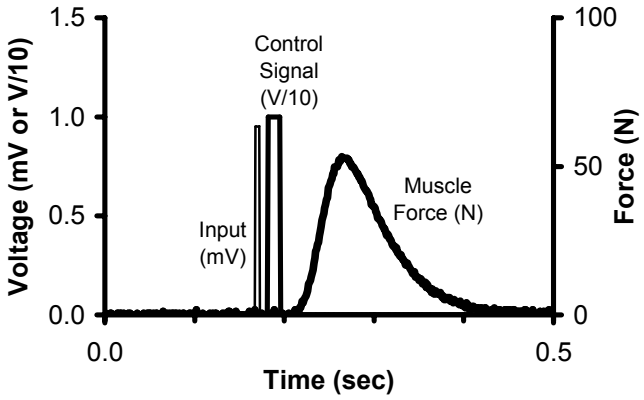

Figure 2. Artificial Muscle Twitch. A 5 ms Input pulse triggered a Control Signal to the proportional pressure regulator, resulting in an artificial muscle twitch. We elicited the twitches during isometric bench top tests.

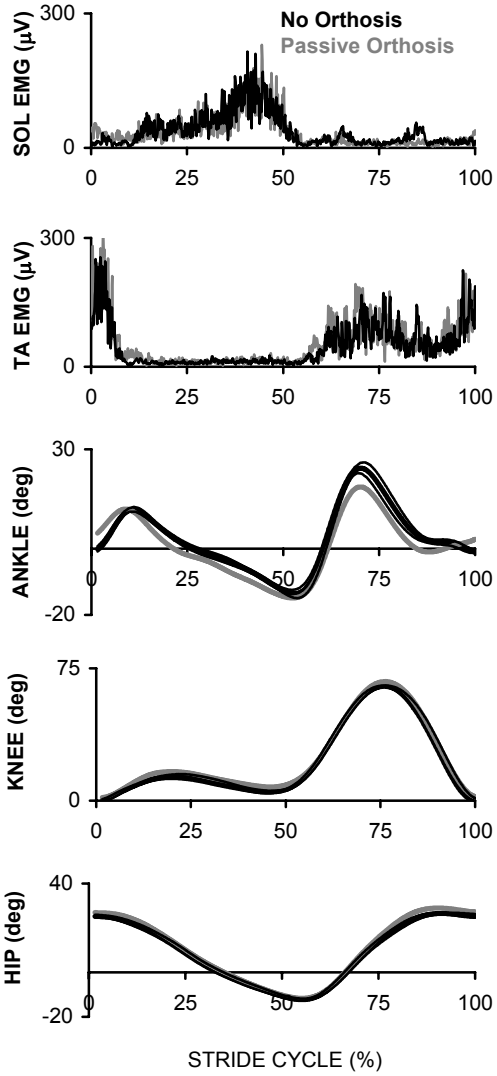

Figure 3. Comparison of muscle activation patterns and joint kinematics for no orthosis and passive orthosis conditions. Mean EMG and joint angle profiles were not substantially different between walking with no orthosis (black lines) and walking with the passive orthosis (grey lines). The most noticeable difference was slightly less dorsiflexion during swing when wearing the passive orthosis. EMG graphs include mean profiles of both conditions. Joint angle graphs include mean profiles of the no orthosis condition (±1 S.D.) and mean profiles of the passive orthosis condition. Zero degrees represents standing posture. Flexion is positive for the knee and hip joint graphs. Plantar flexion is positive for the ankle joint graph.

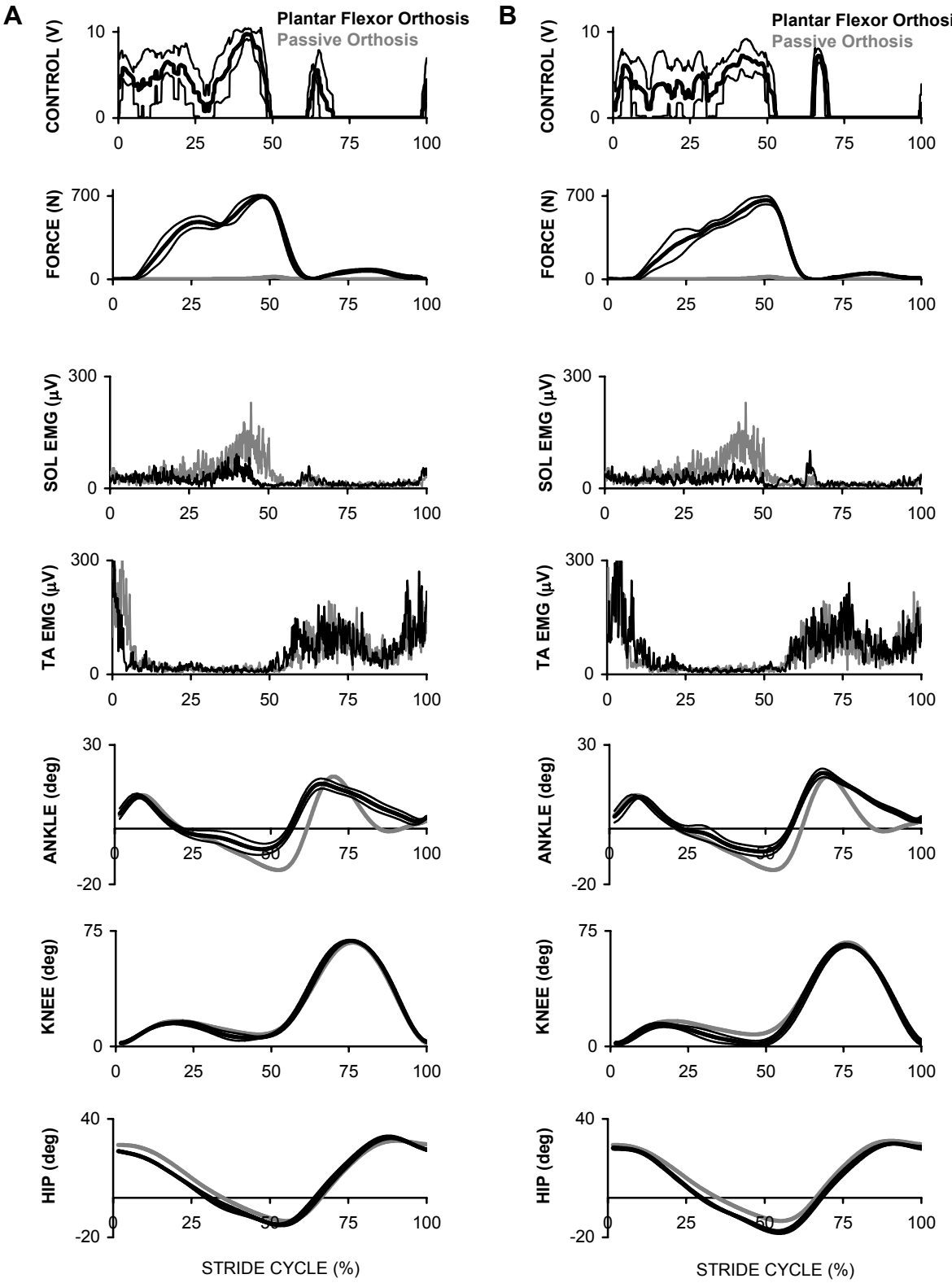

Figure 4. Comparison of muscle activation patterns and joint kinematics for passive orthosis and powered plantar flexor orthosis conditions. Soleus recruitment produced the Control Signal activating the artificial plantar flexor. Powered condition in A is after one minute of wearing the orthosis and powered condition in B is after 30 minutes of wearing the orthosis (both black lines). Passive condition in both A and B is after 6 minutes of wearing the orthosis (grey lines). Soleus EMG amplitude was substantially lower during walking with the powered plantar flexor compared to during walking with the passive orthosis. The ankle joint underwent less dorsiflexion during late stance when the orthosis was powered by the artificial plantar flexor. EMG graphs include mean profiles of both conditions. Control signal, artificial muscle force, and joint angle graphs include mean profiles of the powered orthosis condition (±1 SD) and mean profiles of the passive orthosis condition. Zero degrees represents standing posture. Flexion is positive for the knee and hip joint graphs. Plantar flexion is positive for the ankle joint graph.

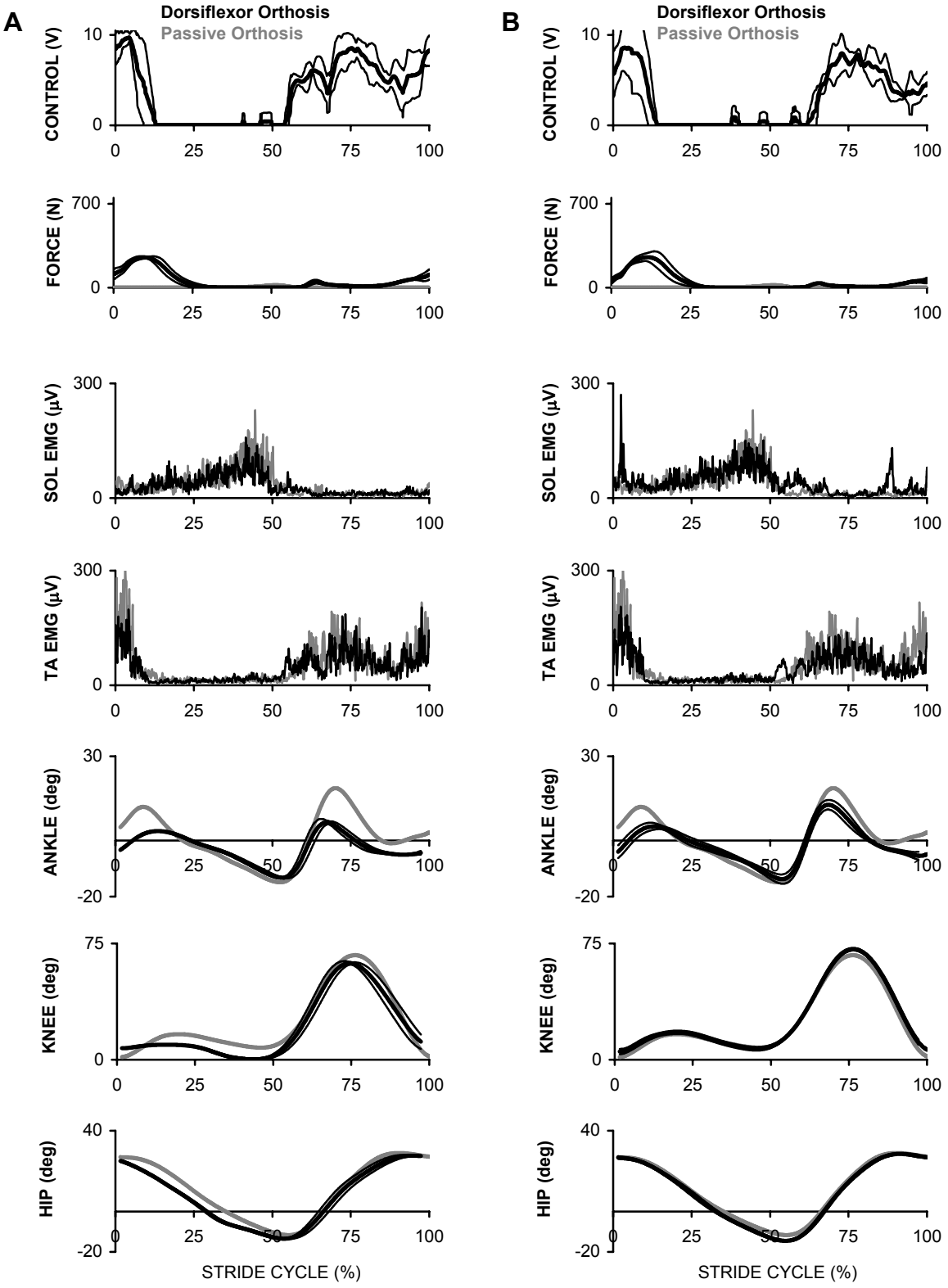

Figure 5. Comparison of muscle activation patterns and joint kinematics for passive orthosis and powered dorsiflexor orthosis conditions. Tibialis anterior recruitment produced the Control Signal activating the artificial dorsiflexor. Powered condition in A is after one minute of wearing the orthosis and powered condition in B is after 30 minutes of wearing the orthosis (both black lines). Passive condition in both A and B is after 6 minutes of wearing the orthosis (grey lines). Tibialis anterior EMG amplitude was slightly lower during walking with the powered dorsiflexor compared to during walking with the passive orthosis. The ankle joint underwent less plantar flexion during early stance and early swing when the orthosis was powered by the artificial dorsiflexor. EMG graphs include mean profiles of both conditions. Control signal, artificial muscle force, and joint angle graphs include mean profiles of the powered orthosis condition (±1 SD) and mean profiles of the passive orthosis condition. Zero degrees represents standing posture. Flexion is positive for the knee and hip joint graphs. Plantar flexion is positive for the ankle joint graph.

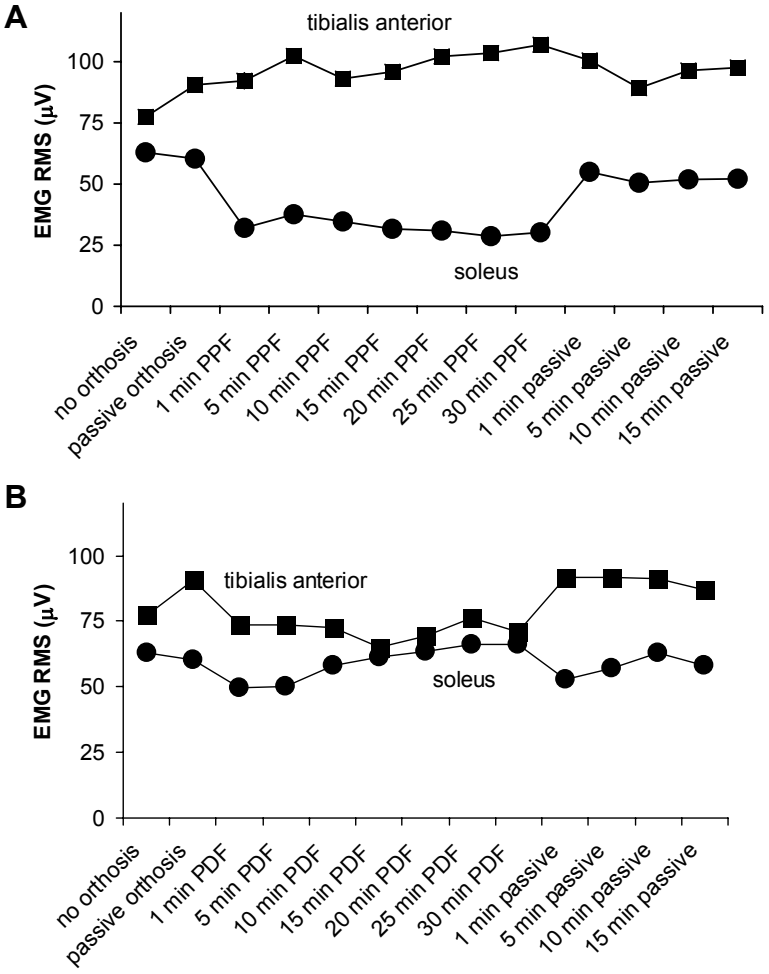

Figure 6. Muscle activation amplitudes. A) During walking with powered plantar flexion (PPF), soleus EMG (circles) decreased to approximately one half the value seen during the passive orthosis condition. Tibialis anterior EMG (squares) remained fairly stable, with only a small increase during powered plantar flexion compared to passive orthosis walking. Both muscles returned quickly to the baseline amplitudes after the orthosis was turned off. B) During walking with powered dorsiflexion (PDF), tibialis anterior EMG (squares) decreased slightly compared to the passive orthosis condition. Soleus EMG (circles) did not change much during powered dorsiflexion compared to walking with the passive orthosis. Points represent the average root mean square amplitude (RMS) of five consecutive stride cycles. Standard error bars are smaller than the symbols.